

Particle image velocimetry image processing to assess cell distribution within bioreactors

Michele Pistillo^{1,*†}, Margherita Scamarcio^{1†}, Federica Liguori^{1†},
Maurizio Mastantuono^{1†}, Simona Gramazio^{2†}, Alfredo Ambrico^{3†},
Rosaria Alessandra Magarelli^{3†}, Maria Martino^{3†}, Mario Trupo^{3†}, Miriam Merco^{4†},
Mario Ledda^{4†} and Giuseppe Falvo D'urso Labate^{1†}

¹Cellex Srl, Piazzale delle Belle Arti, 2 00196 Rome, Italy

²AKKA Technologies Italy, Life Sciences division, via Enrico Tazzoli 215/12b 10137 Torino

³Italian National Agency for New Technologies, Energy and Sustainable Economic Development (ENEA), Trisaia Research Centre SS 106 Jonica, Km 419+500, 75026 Rotondella (Matera), Italy

⁴Institute of Translational Pharmacology, National Research Council (CNR), Via Fosso del Cavaliere 100, 00133 Rome, Italy

Abstract

Cell cultures suspended in bioreactors in a fluid environment are the basis for cell expansion and important medical products manufacturing. Assessing local cell distribution within bioreactors may provide information to increase cell production efficiency. Hydrodynamics characterizations of bioreactors are typically performed via Particle Image Velocimetry (PIV) with fluorescent polystyrene microspheres or Computational Fluid Dynamics (CFD), while local cell distribution is monitored through expensive sensors or direct sampling. However, PIV and CFD analysis lack of cell behaviour representativity, while direct sampling give average and local information and may impact cell culture conditions. In this study a novel non-invasive method, focusing on the optical investigation of suspended fluorescent nanoparticles (NPs) -labelled Chinese hamster ovary (CHO) cells distribution within SUSPENCE® bioreactor through PIV image processing, is presented. Our investigation showcases the favourable effect of an innovative NPs internalisation approach in terms of cellular uptake efficiency and fluorescence brightness. Moreover, NPs-labelled CHO cells (NP-CHO) PIV image processing and analysis robustness is validated by cell sampling and sample processing. Furthermore, the turbulent kinetic energy distribution to gain insight of the impact of hydrodynamic conditions on cell culture is evaluated.

Keywords

Biomedical image processing, Particle Image Velocimetry, Bioreactors, Nanoparticles

DETERMINED 2022: Neurodevelopmental Impairments in Preterm Children – Computational Advancements, August 26, 2022, Ljubljana, Slovenia

*Corresponding author.

† These authors contributed equally.

✉ michelepistillo94@gmail.com (M. Pistillo); margherita.scamarcio@cellex.it (M. Scamarcio); federica.liguori@cellex.it (F. Liguori); maurizio.mastantuono85@gmail.com (M. Mastantuono); Simona.GRAMAZIO@akka.eu (S. Gramazio); alfredo.ambrico@enea.it (A. Ambrico); rosaria.magarelli@enea.it (R. A. Magarelli); maria.martino@enea.it (M. Martino); mario.trupo@enea.it (M. Trupo); Miriam.merco.15@gmail.com (M. Merco); mario.ledda@ift.cnr.it (M. Ledda); management@cellex.it (G. Falvo D'urso Labate)

ORCID 0000-0002-8487-9723 (A. Ambrico); 0000-0001-5419-62543 (R. A. Magarelli); 0000-0002-2640-050X (M. Trupo)



© 2022 Copyright for this paper by its authors. Use permitted under Creative Commons License Attribution 4.0 International (CC BY 4.0).

CEUR Workshop Proceedings (CEUR-WS.org)

1. Introduction

Bioreactors have become fundamental devices in the biomedical industry since they are employed in different fields such as tissue engineering and cell-based therapies [1]. The use of bioreactor for suspension cells culture gives many potential advantages over the static cell culture, including homogeneity of cell conditions, possibility of sampling, automated systems for controlling parameters such as pH, temperature and dissolved oxygen concentration, thus allowing to obtain very high cell densities [2].

Assessing cell and nutrients distribution and fluid flow field is important to evaluate bioreactors performances. In this regard, in the current study turbulent kinetic energy (TKE), a fluid dynamic parameter, and cell concentration distribution have been determined. A homogeneous distribution of all components inside bioreactors, including cells, is a key property to promote nutrients exchange and to avoid cell deposition and local cell accumulation, thus increasing cell growth [3]. On the other hand, TKE is a fluid parameter often employed to evaluate bioreactors mixing mechanisms [4]. As regards to evaluate fluid flow field inside bioreactors, Particle Image Velocimetry (PIV) is a technique used to investigate fluid parameter such as flow pattern information, velocity field and local energy dissipation rates. PIV experimentations are usually conducted using a fluid model composed by water and specific fluorescent tracking particles. Also, through PIV it is possible to study the fluid dynamic characteristics inside bioreactors for cell culture [4]. However, even though tracking particles may possess the same size and density of living cells they not have the same biological properties, so they are unable to mimic the cell behaviour inside cell culture chambers.

Premature new-born children strongly risk to develop health problems in childhood and adolescence, early diagnostics are fundamental to prevent and ensure the welfare of the child [5]. Different cell types can be analysed in newborns, for instance studies have shown the role of nasal epithelial cells in neonates with asthma and allergic rhinitis and so their impact on respiratory disease in adulthood [6]. Another example is represented by peripheral blood mononuclear cells from umbilical cord blood of premature born babies, that can be cultured in bioreactors for suspended cell culture and that can be employed to investigate inflammatory processes that are a cornerstone of pathophysiology in the developing organs of preterm born children [7][8]. As it is reported in the mentioned studies, the improvement in cell culture through the employment of bioreactors will lead to obtain a higher number of cells and a higher amount of biomolecules production compared to static cell culture, thus facilitating the downstream early diagnosis processes for preterm new-borns. In the current study, CHO cells were tested with the possibility of extending the same analysis to other cell types.

In this study a novel non-invasive method has been developed, focusing on the optical investigation of suspended fluorescent nanoparticles (NPs) -labelled Chinese hamster ovary (CHO) cells distribution within SUSPENCE® bioreactor, through PIV image processing. PMMA-FluoRed-COOH NPs were internalized by CHO cells and the experiments were conducted using cell culture medium as the liquid phase. Moreover, NPs-labelled CHO cells (NP-CHO) distribution analysis robustness was confirmed by comparing it to direct cell sampling measurements.

The current work is structured as follows. Section 2.1 describes how cell culture was performed, both in static and in dynamic conditions. In section 2.2 cell label techniques and NPs internalisation inside cells methods are presented (results reported in Section 3.1). In section 2.3

the experimental setup used for PIV images acquisition of NP-CHO, including bioreactor set up and PIV system description, are reported. Section 2.4 describes the techniques used for PIV-images post processing: firstly the algorithm used for background noise reduction and then the methods employed for cell and TKE distribution estimation (results reported in Section 3.2).

2. Materials and Methods

2.1. Cell culture

In recent years, NPs have gained increasing interest in various research fields, especially in the biotechnological and biomedical fields [9]. Moreover, fluorescent NPs can be internalised by living cells, and their uptake can be assessed via fluorescence microscopy, at the same light wavelength emitted by tracer particles used for PIV analysis [10] [9]. Methods to obtain NPs internalisation within CHO cells growth in adherence can be easily found in literature [11]. For these reasons, and since the aim of this work was to study cell distribution within a bioreactor for cell growth in suspension via PIV, we choose to use NPs to label CHO cells, firstly starting from CHO's growth in adherence and subsequently with CHO's growth in suspension.

2.1.1. Adherence cell culture

CHO cells (American Type Culture Collection) were grown in Corning® TC-Treated Multiple Well Plates using Ham's F-12K (Kaighn's) medium supplemented with 10 % heat-inactivated fetal bovine serum (FBS, Euroclone), 2 mM L-glutamine (Sigma), 1.0 unit ml⁻¹ penicillin (Sigma), and 1.0 mg⁻¹ streptomycin (Sigma). The cell line was cultured on a plastic Petri dish at 37°C in a humidified incubator containing 5% CO₂.

2.1.2. Suspension cell culture

The content of one vial from the cryopreserved CHO cell bank was thawed and suspended in 80 mL pre-warmed CD FORTI CHO medium (Thermo Fisher) supplemented with 4 mM L-glutamine (Biowest, France) and 1% Penicillin/Streptomycin (GE Healthcare Bio-Sciences, Sweden). The CHO suspension was grown in ventilate Erlenmeyer flask and kept in a shaker incubator (80-85 RPM) at 37°C and with 5-7% CO₂ for 96 hours.

2.2. Cell labelling and nanoparticles internalisation inside cells

2.2.1. Fluorescent nanoparticles cell internalisation

Red-fluorescent monodisperse polymethylmethacrylate carboxylated particles (microParticles GmbH, Germany) with a mean diameter of 286 nm (PMMA-FluoRed-COOH, SD = 7nm, abs/em = 530/607 nm, COOH >30 µmol/g) were used to stain cells. The internalisation of NPs in CHO cells grown in adherence was performed as follow: firstly, cells were seeded in a Corning® TC-Treated Multiple Well Plates, where each well contained 3mL of suspended cells at a cell concentration of $8,33 \cdot 10^5$ cells/mL. A 0,0025 g/mL NPs starting solution was obtained by diluting PMMA-FluoRed-COOH stock solution at room temperature with cell culture medium.

0,1 mL of starting solution were added to each well to obtain a NPs concentration of 68000 NPs/cell, expressed also as $1,7 \cdot 10^{12}$ NPs/mL and 83,3 $\mu\text{g/mL}$, the latter comparable to NPs concentration values for cell internalisation found in literature [12]. Cells were incubated for different time periods (1 hour, 3 hour and overnight) under growth conditions in order to identify proper incubation periods to maximize the number of internalised NPs. Then, cell medium containing residual NPs was discarded and cells were washed thrice with Dulbecco's phosphate buffered saline (DPBS). DNA staining was performed by using Hoechst dye (Thermo Scientific™ Solution Hoechst 33342) 20 nM. Cells were harvested with 0.05% trypsin/EDTA 1 × and via centrifugation (980 RPM, 5 minutes) and suspended in fresh cell culture medium. Finally, NPs-labelled cells (NPs-CHO) were examined using a fluorescence microscope (Olympus IX51, RT Slider SPOT—Diagnostic Instruments, Sterling Heights, MI, USA), equipped with a 20 × objective and with a cooled CCD camera (Spot RT Slider, full frame; Diagnostic Instruments). Moreover, the effect of fluorescence microscope exposition time (10, 100 and 1000 ms) on images quality, intended as the easiness for the user to recognise NPs inside cells, was qualitatively evaluated.

Regarding suspended CHO cells, a different method was developed and used to ensure NPs internalisation. Firstly, PMMA-FluoRed-COOH NPs working solution at the same concentration used for adherent cells internalisation (as mentioned above: 68000 NPs/cell; $1,7 \cdot 10^{12}$ NPs/mL NPs/mL; 83,3 $\mu\text{g/mL}$) was obtained by diluting PMMA-FluoRed-COOH NPs stock solution in fresh cell culture medium. CHO cells were seeded and expanded in suspension cell growth conditions, and when the required cell number was reached, they were harvested via centrifugation (700 RPM - 6 minutes) and re-suspended in PMMA-FluoRed-COOH NPs working solution, transferred into a T175 Corning® cell culture flasks (Falcon) and incubated at different time periods in static condition. Then, cells were washed thrice via centrifugation (700 RPM - 6 minutes) and re-suspended in fresh cell culture medium. Images of fluorescent nanoparticles labelled – suspended CHO cells (NPs-SCHO) were collected using a fluorescence microscope (Nikon Eclipse E400) with B-2A filter (Ex=450-490, DM=500, BA=515).

In order to compare the effect of NPs encapsulation in terms of fluorescence intensity to different cell staining procedures, NPs-SCHO fluorescence intensity was compared to the one of CHO cells stained with CellTracker®Orange probe (Invitrogen, UK), a largely used cell dye [13] [14].

2.2.2. CellTracker® staining

Cell staining was performed, according to manufacturer's protocols, by using CellTracker® Orange probe (Invitrogen, UK). 10 mM CellTracker® Orange (Invitrogen, UK) stock solution was prepared by dissolving CellTracker® in high-quality, anhydrous dimethylsulfoxide (DMSO). 25 μM staining solution was obtained diluting stock solution to CD FORTI CHO medium. The working solution was added to suspended cells after harvesting them via centrifugation (700 RPM, 6 minutes), and cells were incubated for 45 minutes under growth conditions. Then, the working solution was replaced with fresh media and the cells were examined using two fluorescence microscope, depending on the laboratory availability: (i) Nikon Eclipse E400 with B-2A filter (Ex=450-490, DM=500, BA=515) and (ii) Olympus IX51, RT Slider SPOT equipped with a 20 × objective and with a cooled CCD camera Spot RT Slider, full frame, Diagnostic Instruments USA).

2.3. Experimental set up for PIV images acquisition

2.3.1. Bioreactor set up

Suspence® (Cellex, Italy) was the bioreactor used in this work: it consists of a device in which cell culture fluids are continuously pumped in its semi-transparent vessel from the bottom and exit from an outlet in the upper part. Cell suspension in CD FORTI CHO medium (Thermo Fisher) supplemented with 4 mM L-glutamine (Biowest, France) and 1% Penicillin/Streptomycin (GE Healthcare Bio-Sciences, Sweden) was inoculated in the bioreactor with a starting volume of 1500 mL, at a starting density of $5 \cdot 10^5$ cells/mL, where the 5% of the total were NPs-SCHO cells. Medium perfusion was guaranteed by using a peristaltic pump (MASTERFLEX® L/S® 07522-20) setting a flow of 80 mL/min. Figure 1 illustrates the inner geometry of Suspence® vessel. Cell samples were withdrawn at different time points after the cell seeding (30, 180 and 300 minutes) in three different areas inside the bioreactor: the "Bottom" area, located approximately near the bottom inner surface of the vessel, the "Centre" area, at approximately 70 mm from the bottom, and the "Top", located near the liquid free surface.



Figure 1: 3D rendering of the inner geometry of the vessel of Suspence® bioreactor. Cells are seeded inside the vessel and they move from the bottom part to the top.

2.3.2. PIV acquisition system

Suspence® bioreactor was positioned inside a parallelepipedal glass tank filled with distilled water, to reduce errors caused by refractive and diffractive light phenomena on the cylindrical surface of the bioreactor. PIV analysis were carried out by employing planar PIV system (Dantec Dynamics, Denmark) with a green laser (Dantec Dynamics, Denmark) providing a light beam of 532 nm and a Flow Sense USB camera (Dantec Dynamics, Denmark). The camera was

positioned perpendicularly to the laser beam. Figure 2 illustrates the PIV acquisition system and the bioreactor configuration for PIV images acquisition employed during this work.



Figure 2: PIV system and the bioreactor configuration for images acquisition employed during this work. The Suspence® bioreactor was positioned inside a glass tank filled with distilled water to reduce refractive and diffractive light phenomena. A green laser and a camera (Dantec Dynamics, Denmark), positioned perpendicularly to the laser beam, were also used.

Planar images for cell distribution were acquired at nine different levels of frontal plane of the bioreactor, with the first level located at the zone in direct contact with the bottom surface of the bioreactor and the last level covering the sections next to the free surface of the cell suspension and the bioreactor outlet. A Cartesian coordinate system was used, with the vertical and horizontal coordinates indicated respectively by y and x . The system origin was located at the left end of the bioreactor bottom inner surface. The laser was oriented to acquire the horizontal and vertical direction of cells' speed. Figure 3 illustrates the spatial distribution of the nine investigated sections. Images length along the y -axis was approximately 6 mm, while images width along the x -axis ranged from 45,7 to 49,1 mm, corresponding to the laser-illuminated area dimensions. Laser beam thickness was approximately 1 mm.

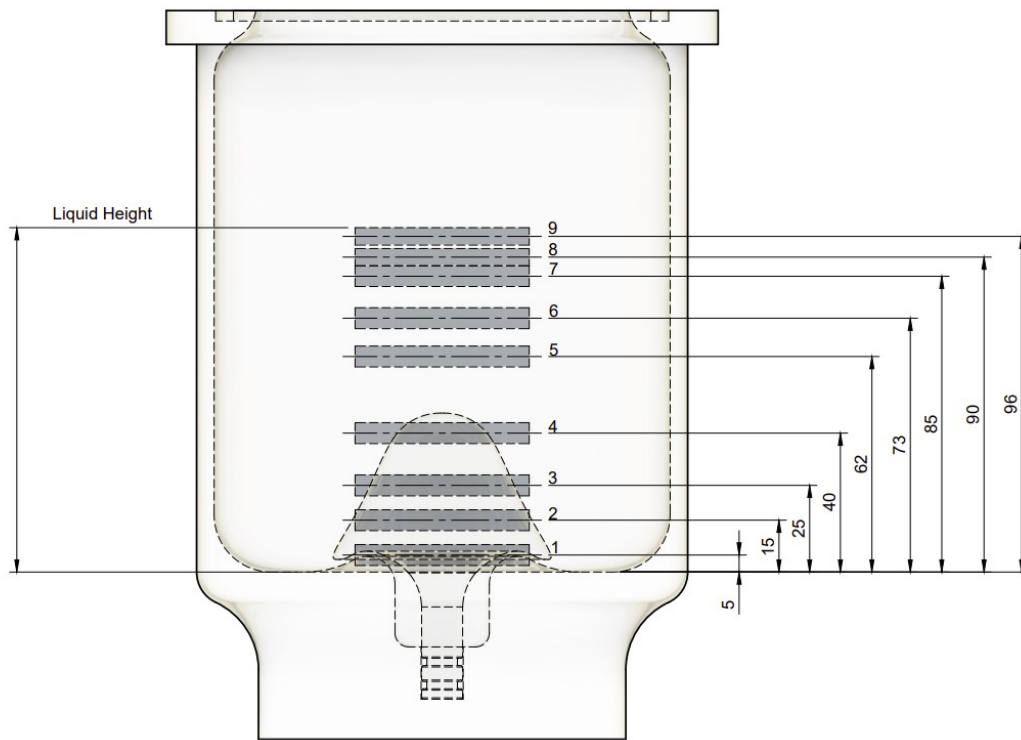


Figure 3: Spatial distribution of the nine planar sections investigated via PIV. These sections were analysed in order to evaluate cell distribution and flow speed along all the vessel height. Section vertical length is approximately 6 mm, while horizontal width ranges from 45,7 to 49,1 mm. Dimension on the right are expressed in millimeters.

2.4. PIV images post processing

2.4.1. PIV images background noise removal

A Dantec Dynamic PIV system was used to acquire the images in the vertical plane; nine sections, as shown in Figure 3, were recorded and at different time points. For each condition 100 images, subsequently used for TKE distribution estimation, were taken and imported into Python to estimate the percentage of cells in suspension. Two images for each section were analysed at a time. Background noise removal is fundamental for biomedical image processing [15]. During the PIV images post processing the background noise, caused by the presence of refractive and diffractive light phenomena, was reduced by using a Python script. In our application the MedianBlur value, obtained computing the median of all pixels under the kernel window and the central pixel, represented the background noise, since noise corresponded with a diffuse background halo. Different kernel size, consisting in the product between the filter mask width and height in pixels, were used (7x7, 11x11, 15x15, 21x21) [16]. Thus, the background value was subtracted from the starting images. The subtraction was performed because the significant content of PIV images was assumed to be the single pixel value, that represented the absence

or the presence of single or aggregate cells. The threshold binary function was also used to separate even more the objects (NPs-SCHO) considered as a foreground from its background. In brief, the images were modified by this function so that all pixel intensity values higher than the threshold were assigned the maximum value (white), or the minimum value (black). More specifically, when pixel values were greater or equal than the set threshold value (50 or 100), they were set to 255, in the other case they were set to 0 (black) [17]. Basic Python libraries have been used, such as “cv2” to read images, “numpy” for scientific computing and “matplotlib” to plot images.

2.4.2. Cell distribution estimation

For each of the nine sections, the number of nonzero pixels of the two images was determined, and the result of the mean between these numbers gave an estimation of the amount of cells in suspension. PIV image processing and analysis robustness was assessed by comparing it to cell distribution analysis carried out via cell sampling and sample processing. Since three cell sampling points were used, three mean areas close to the point where cells were withdrawn were investigated. These three areas, which account for cell distribution in the bottom, centre and upper part of the bioreactor, were named “Bottom”, “Centre” and “Top” and represented respectively the mean between values measured in section (1, 2, 3), (4, 5) and (6, 7, 8, 9). For each area, values were normalised to the total value, equal to the sum of the total values of the three areas, calculated at time 0 (cell seeding into the bioreactor). The results were shown as bar graphs and compared with values obtained from the 3 cell samples. Total cell counts were determined by hemocytometer, as Bürker chamber, using a fluorescence microscope. The cell samples and the images acquired by the PIV system and post-processed with the above-mentioned Python Script were taken at different time points after bioreactor seeding (30, 180 and 300 minutes).

2.4.3. Ensemble-averaged turbulent kinetic energy distribution analysis

TKE is an index that can be employed to understand mass transfer and cell viability within bioreactors [18] [19] [20]. TKE distribution was obtained by re-adapting a previous PIV data processing method developed by Odeleye et. al. [10]. Measurements were carried out with a bioreactor fill volume of 1500 mL and at a flow rate of 80 mL/min. For each frontal plane section of the bioreactor, 100 image pairs were collected to obtain 100 instantaneous NPs-SCHOs velocity components (along the x and y axis) vector maps. The two components along the x and y axis of NPs-SCHOs velocity from the PIV measurements were calculated employing the adaptive PIV processing algorithm provided within Dynamic Studio software (Dantec Dynamics, Denmark). Interrogation areas were set from 16x16 to 32x32 pixels, while a universal outlier detection in neighbourhoods of 5x5 pixels was used for validating vectors. For velocity gradient adaptivity, the absolute value of each component of the velocity gradient was limited to 0.1 while the total magnitude of the gradients (square root of the sum of the squares) was limited to 0.2. Spatial resolution obtained within vector maps ranged between 0.4 x 0.4 and 0.48 x 0.48 mm. The mean value between vector maps was calculated in order to obtain vector maps representing the “Bottom”, “Centre” and “Top” areas respectively between velocity values calculated in section (1,

2,3), (4, 5) and (6, 7, 8, 9). These were post-processed by using a second Python script to obtain the ensemble-averaged turbulent kinetic energy through equations presented by Odeleye et. al. [10]. Since in the latter work kinetic energy was divided to the square of spinner tip speed and Suspence® bioreactor does not have an impeller, in this work turbulent kinetic energy has been divided to the square of the input fluid speed. For simplicity, turbulent kinetic energy distribution was normalised to the maximum value found in all the investigated frontal plane levels.

Figure 4 illustrates the steps, from the acquisition one to those executed in the post processing phase, performed in this work.

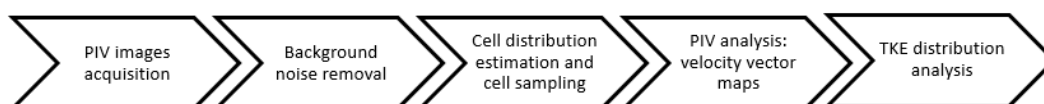


Figure 4: Schematics of PIV images acquisition and post processing steps performed in this work.

3. Results and discussion

3.1. Fluorescent cell labelling

PMMA-FluoRed-COOH NPs uptake in CHO was monitored via fluorescence microscope (Figure 5). Images show that, at each investigated incubation time, NPs appear to be localised around cell nuclei, and this may reveal that NPs were able to accumulate within cells. Also, Figure 5 shows that the number of red spots around cell nuclei tend to increase over incubation time, to such an extent that after incubating cells overnight, red fluorescence light appears to be predominant (Figure 5c). In this case, NPs can be considered internalised since some nuclei appear to be purple due to light overlap. For these reasons, NPs incubation time was subsequently set at 10 hours. These findings may suggest that the internalised NPs number increase over incubation time. This result is in line with findings shown by dos Santos et. al. [12]. Further studies are needed to fully understand the internalisation mechanisms.

Figure 6 shows PMMA-FluoRed-COOH NPs uptake in CHO cells at three different exposure times. As can be recognised from these images, an exposure time of about 100 ms was considered suitable to assess NPs internalisation.

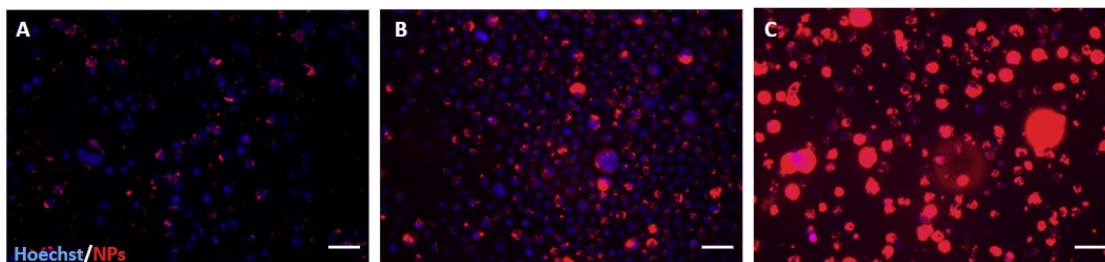


Figure 5: Internalisation evaluation of PMMA-FluoRed-COOH NPs inside CHO cells (NPs-CHO) via fluorescence microscope at different incubation times under cell culture conditions: (A) 1 hour, (B) 3 hours and (C) overnight. Cells nuclei were stained in blue while NPs are visualised in red. Exposition time: 1000ms. Scale bar = 100 μm .

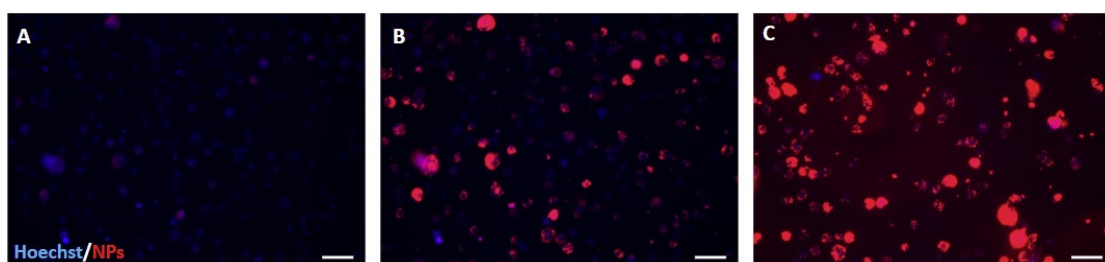


Figure 6: Internalisation of PMMA-FluoRed-COOH NPs inside CHO cells (NPs-CHO) evaluation performed via fluorescence microscope at different exposition times: (A) 10 ms, (B) 100 ms and (C) 1s. Cell nuclei were stained in blue while NPs are visualized in red. Scale bar = 100 μm .

Figure 7A illustrates CHO cells stained with cell tracker CellTracker®. In this case, few cells, shown as red spots, can be distinguished (e.g in the upper-right corner of the image). Figure 7B shows PMMA-FluoRed-COOH NPs uptake in CHO cells. In order to compare the results, the incubation time for NPs encapsulation was set to 1 hour (similar to the incubation time set for CellTracker dye, 45 min). From these images the difference in the obtained fluorescence intensity between the two used methods is appreciable, with the NPs-CHO cells fluorescence being more intense than CellTracker® one. Further quantitative fluorescence intensity analysis are needed to confirm this result.

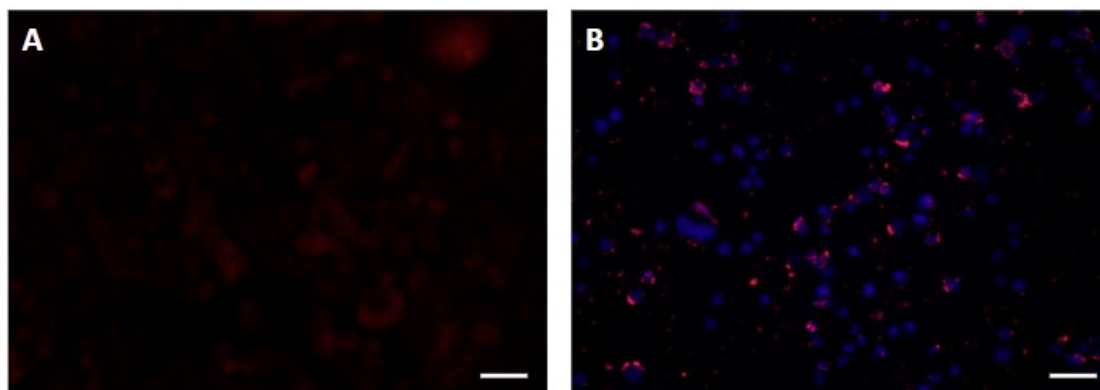


Figure 7: Comparison of the fluorescence intensity obtained via CellTracker® cell dye staining and via NPs internalisation. (A) CHO cells stained with CellTracker® (Incubation Time: 45 minutes), cells are visualized as red spots and (B) PMMA-FluoRed-COOH NPs inside CHO cells (NPs-CHO), cells nuclei were stained in blue while NPs are visualized in red (Incubation time: 1 hour). Images were acquired via fluorescence microscope. Exposition time: 100 ms. Scale bar = 100 μ m.

3.1.1. Fluorescent nanoparticles internalisation in cells growth in suspension

The effectiveness of the new method developed to ensure NPs internalisation within CHO cells growth in suspension was demonstrated by comparing fluorescence intensity of CHO cells growth in adhesion stained with CellTracker® (Figure 8A) to the one emitted by NPs-SCHO (Figure 8B). These images provide evidence that cells can be clearly distinguished with both methods. Also, fluorescence intensity of NPs-SCHO appears to be comparable to CellTracker® one. Further quantitative fluorescence intensity analysis is needed to confirm this result.

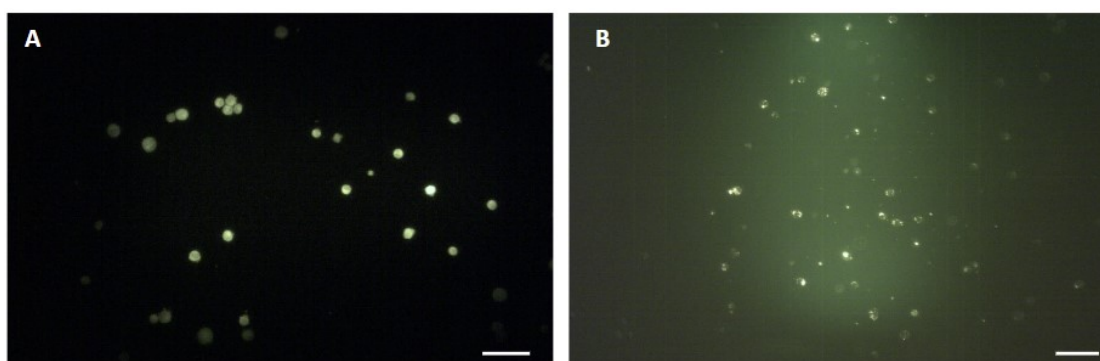


Figure 8: Evaluation of the NPs internalisation within CHO cells growth in suspension in terms of fluorescence intensity. Fluorescence microscope images: (A) CHO cells growth in adhesion stained with CellTracker®: cells are visualized in green and (B) PMMA-FluoRed-COOH NPs inside CHO cells growth in suspension (NPs-SCHO), NPs are visualized in green too. Incubation time: overnight. Exposition time: 69 ms. Scale bar = 50 μ m.

3.2. PIV images post processing

3.2.1. PIV images background noise removal

Section three of one of the nine sections acquired using the PIV system was used to evaluate the performance of the developed Python filter and is shown in Figure 9. In this case, the kernel size was set to 21, while the value of the Threshold Binary function was set to 50. Figure 9A, 9B and 9C represent respectively the non-filtered image, the image containing only the background noise, and the filtered image obtained via the employed Python script processing. As can be seen from these figures, the reduction of noise is clearly distinguished on the filtered image (Figure 9C) single fluorescent dot, that can be associated with single cells or cell aggregates, can be distinguished.

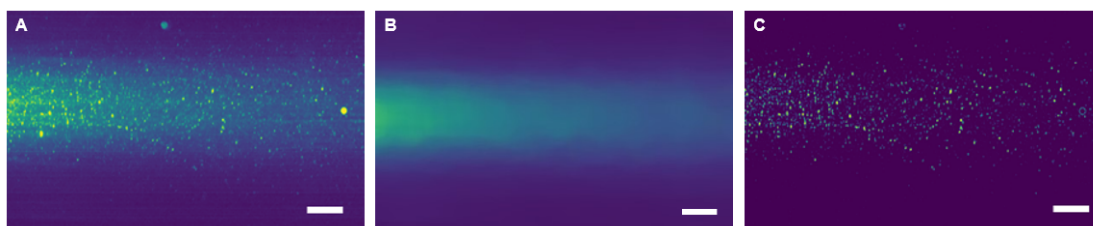


Figure 9: Effect of the background noise removal filter on PIV images of NPs-SCHO within SUSPENCE®. (A) Non filtered PIV image (B) PIV image containing only the background noise and (C) Filtered PIV image using Python script. Analysed section number: 3. Scale bar = 5mm.

3.2.2. Cell distribution estimation

Figure 10 shows cell distribution results obtained via PIV images post processing and via cell sampling. The results of the two different used methods may be considered comparable, especially in the first two time points considered. In addition, a homogeneous distribution of the cell distribution inside the vessel is highlighted, indeed values found in different areas (Bottom, Centre and Top) appear to be similar. After 30 minutes from seeding the percentage of the cell concentration is about 33%, instead after 180 minutes about 34%, in both systems described. This highlights how cell suspension is maintained over time. Anyway, a difference between the two methods can be seen in the last time point considered (300 minutes). In both systems the percentage of cell concentration in the Top area is about 40%. While the Bottom area is about 28% and 32% and the Centre area is about 33% and 27%, in the PIV system and cell samples respectively. This difference may be due to human errors occurring during PIV image acquisition procedures. In the latter case, the measurements obtained from the cell samples are considered more truthful, showing a non homogeneity of the cell concentration inside the vessel.

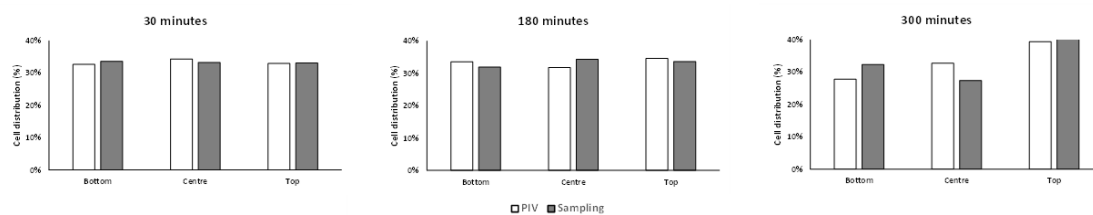


Figure 10: Bar graphs showing cell distribution results obtained via PIV images acquisition and Python script postprocessing (PIV) compared to the one obtained via cell sampling and cell counting (Sampling), at different time points.

3.2.3. Ensemble-averaged turbulent kinetic energy distribution analysis

Figure 11 shows the ensemble averaged turbulent kinetic energy (TKE) distribution of NPs-SCHO in the tree investigated bioreactors areas. A high normalized TKE area can be found in the central region of the Bottom area, corresponding to the region close to the bioreactor inlet. In this area the value of TKE appears to gradually decrease when moving away from the central zone, and this may suggest that the considered area is well mixed, since TKE is considered the portion of kinetic energy that provides a mixing mechanism due to turbulent dispersion [4]. Mixing is fundamental to obtain homogeneity of nutrients and oxygen and to reduce gradients induced by addition of cell culture media and acid/base tirants and to increase mass transfer. However, an increase in turbulent energy may be related to an increase in hydrodynamic stresses that can hinder cell viability [18][19][20]. Another high normalized TKE area is found along the length of the top area, corresponding to the region close to the bioreactor outlet. Differently from the TKE distribution of the bottom area, TKE appears to be high also in the peripheral zones. Moreover, TKE distribution in the Centre zone appears to be similar to the one observed in the bottom zone but with a lower intensity. TKE intensity in this area appears to be higher than the one observed by Odeleye et. al.[10], and this can be associated to a higher mixing mechanism in the central area of the bioreactor and also to the presence of an inlet and an outlet in the Suspence® bioreactor, which are absent in the bioreactor tested in the above-mentioned study.

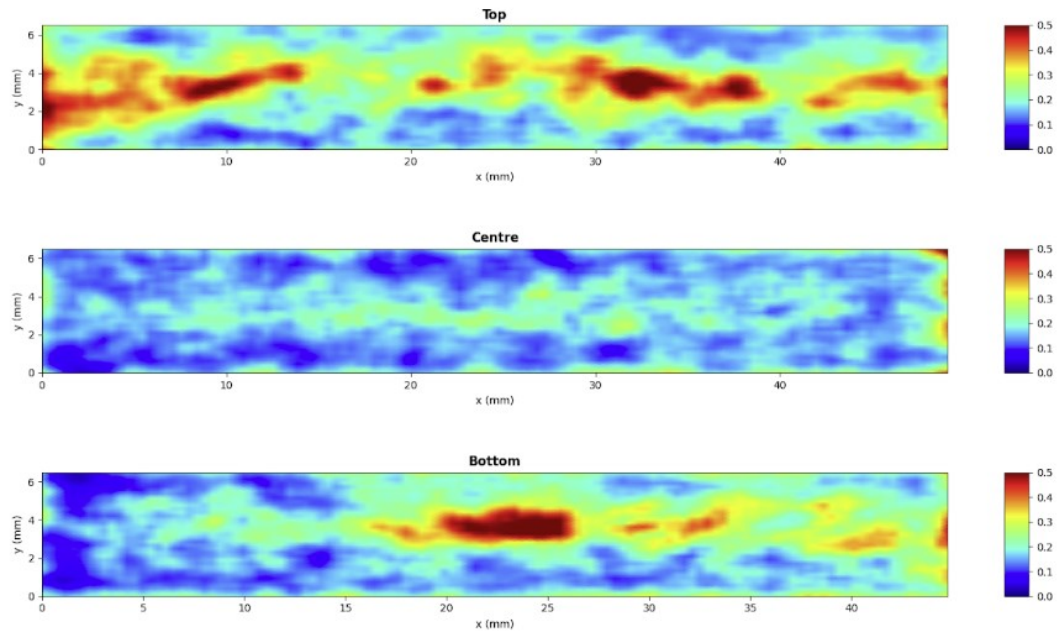


Figure 11: Ensemble-averaged turbulent kinetic energy (TKE) distribution of NPs-SCHO normalized to the maximum TKE value found in the investigated bioreactors areas (Top, Centre, Bottom). TKE is considered the portion of kinetic energy that provides a mixing mechanism, fundamental to obtain homogeneity of nutrients and oxygen. High normalized TKE regions can be seen near the inlet and the outlet of the bioreactor, where flow speed is higher than the rest of the considered volume.

4. Conclusions

In this work we have demonstrated the effectiveness of the new method developed to ensure NPs internalisation within CHO cells growth in suspension and we have exploited NPs-SCHO to study cell and kinetic energy distribution within SUSPENCE® bioreactor via PIV analysis and data processing. Fluorescent particles are typically employed for fluid dynamic characterization of bioreactors and are monitored in different conditions and under various stimuli (e.g. chemico-physical). The ability to internalise fluorescent nanoparticles inside CHO cells allowed the use of the PIV system as a non-invasive image acquisition tool for bioreactors for cell culture in suspension. To the extent of our knowledge, in this work for the first time living cells with encapsulated fluorescent NPs have been employed, instead of tracer particles alone, for PIV analysis. The quantification of cell distribution and hydrodynamic parameters, in the same condition in which the cells are used to grow, within a bioreactor using PIV may allow a complete and strict study upon local cell culture conditions. Regarding PIV images post processing, firstly images background noise was successfully filtered by using our Python Script. Then, a second script was used to calculate cell distribution within the bioreactors. Cell distribution values appeared to be comparable, especially in the first two time points investigated, to the one obtained via cell sampling. The ensemble averaged turbulent kinetic energy (TKE) distribution

of NPs-SCHO was obtained in the three investigated bioreactors areas. High normalised TKE regions were found near the inlet and the outlet of the bioreactor, where flow speed is higher than the rest of the considered volume. Also, in the central area of Suspence® TKE intensity appeared to be higher than the one observed in the same area of other bioreactors. In these regions, mixing of nutrients and oxygen is promoted, but also high levels of TKE may hinder cell viability. Future development would be employing PIV cell distribution and TKE distribution analysis on different types of cells to predict cell distribution and behaviour within bioreactors during longer-lasting cell culture. In conclusion, PIV cell distribution and TKE distribution analysis inside bioreactors may represent two new methods to optimize culture conditions for cells (e.g. Peripheral Blood Mononuclear Cells) used for preterm new-borns diagnosis and therapy.

References

- [1] M. Stephenson, W. Grayson, Recent advances in bioreactors for cell-based therapies, *F1000Research* 7 (2018).
- [2] K. S. Carswell, E. T. Papoutsakis, Culture of human t cells in stirred bioreactors for cellular immunotherapy applications: Shear, proliferation, and the il-2 receptor, *Biotechnology and bioengineering* 68 (2000) 328–338.
- [3] R. Olmer, A. Lange, S. Selzer, C. Kasper, A. Haverich, U. Martin, R. Zweigerdt, Suspension culture of human pluripotent stem cells in controlled, stirred bioreactors, *Tissue Engineering Part C: Methods* 18 (2012) 772–784.
- [4] A. Håkansson, D. Arlov, F. Carlsson, F. Innings, Hydrodynamic difference between inline and batch operation of a rotor-stator mixer head-a cfd approach, *The Canadian Journal of Chemical Engineering* 95 (2017) 806–816.
- [5] A. R. Hayward, Development of lymphocyte responses and interactions in the human fetus and newborn, *Immunological reviews* 57 (1981) 39–60.
- [6] D. Miller, S. W. Turner, D. Spiteri-Cornish, N. McInnes, A. Scaife, P. J. Danielian, G. Devereux, G. M. Walsh, Culture of airway epithelial cells from neonates sampled within 48-hours of birth, *PLoS One* 8 (2013) e78321.
- [7] J. Baier, A. C. Gwellem, R. Haase, I. Volkmer, B. Bartling, M. S. Staeger, Co-culture of peripheral blood mononuclear cells and endothelial colony forming cells from cord blood of preterm born babies, in: *In Vitro Models for Stem Cell Therapy*, Springer, 2021, pp. 107–124.
- [8] P. C. Collins, L. K. Nielsen, S. D. Patel, E. T. Papoutsakis, W. M. Miller, Characterization of hematopoietic cell expansion, oxygen uptake, and glycolysis in a controlled, stirred-tank bioreactor system, *Biotechnology progress* 14 (1998) 466–472.
- [9] A. Bhattacharyya, P. Datta, P. Chaudhuri, B. Barik, Nanotechnology-a new frontier for food security in socio economic development, in: *Disaster risk vulnerability conference*, 2011, pp. 116–120.
- [10] A. Odeleye, D. Marsh, M. Osborne, G. Lye, M. Micheletti, On the fluid dynamics of a laboratory scale single-use stirred bioreactor, *Chemical Engineering Science* 111 (2014) 299–312.

- [11] V. B. Bregar, J. Lojk, V. Šuštar, P. Veranič, M. Pavlin, Visualization of internalization of functionalized cobalt ferrite nanoparticles and their intracellular fate, *International journal of nanomedicine* 8 (2013) 919.
- [12] T. Dos Santos, J. Varela, I. Lynch, A. Salvati, K. A. Dawson, Quantitative assessment of the comparative nanoparticle-uptake efficiency of a range of cell lines, *Small* 7 (2011) 3341–3349.
- [13] O. Uckermann, I. Iandiev, M. Francke, K. Franze, J. Grosche, S. Wolf, L. Kohen, P. Wiedemann, A. Reichenbach, A. Bringmann, Selective staining by vital dyes of müller glial cells in retinal wholemounts, *Glia* 45 (2004) 59–66.
- [14] M. Hsu, T. Andl, G. Li, J. L. Meinkoth, M. Herlyn, Cadherin repertoire determines partner-specific gap junctional communication during melanoma progression, *Journal of cell science* 113 (2000) 1535–1542.
- [15] S. R. Sternberg, Biomedical image processing, *Computer* 16 (1983) 22–34.
- [16] B. Chen, J. Liang, N. Zheng, J. C. Príncipe, Kernel least mean square with adaptive kernel size, *Neurocomputing* 191 (2016) 95–106.
- [17] S. Parveen, J. Shah, A motion detection system in python and opencv, in: 2021 third international conference on intelligent communication technologies and virtual mobile networks (ICICV), IEEE, 2021, pp. 1378–1382.
- [18] S. Mishra, V. Kumar, J. Sarkar, A. S. Rathore, Cfd based mass transfer modeling of a single use bioreactor for production of monoclonal antibody biotherapeutics, *Chemical Engineering Journal* 412 (2021) 128592.
- [19] A. Nienow, *Hydrodynamics of stirred bioreactors* (1998).
- [20] A. R. Lara, E. Galindo, O. T. Ramírez, L. A. Palomares, Living with heterogeneities in bioreactors, *Molecular biotechnology* 34 (2006) 355–381.